

Structure, Luminescence, and Adsorption Properties of Two Chiral Microporous Metal–Organic Frameworks

Qianrong Fang, Guangshan Zhu,* Ming Xue, Jinyu Sun, Fuxing Sun, and Shilun Qiu*

State Key Lab of Inorganic Synthesis & Preparative Chemistry, Jilin University, Changchun 130012, People's Republic of China

Received October 20, 2005

Two 3D chiral multifunctional microporous MOFs, $Zn_3(BTC)_2(DMF)_3(H_2O) \cdot (DMF)(H_2O)$ (**1**) and $Cd_4(BTC)_3(DMF)_2 \cdot (H_2O)_2 \cdot 6(H_2O)$ (**2**) ($H_3BTC = 1,3,5$ -benzenetricarboxylic acid and $DMF = N,N$ -dimethylformamide), have been synthesized in the presence of organic bases tributylamine (TBA) and triethylamine (TEA), respectively. **1** ($C_{30}H_{38}N_4O_{18}Zn_3$) crystallizes in the tetragonal $P4_12_12$ space group ($a = 13.6929(19)$ Å, $c = 50.664(10)$ Å, $V = 9499(3)$ Å³, and $Z = 8$). **2** ($C_{33}H_{39}N_2O_{28}Cd_4$) crystallizes in the tetragonal $P4_322$ space group ($a = 10.3503(4)$ Å, $c = 52.557(3)$ Å, $V = 5630.4(4)$ Å³, and $Z = 4$). X-ray crystallography reveals that **1** consists of a 3D open framework with the $(6^3)_4(6^2 \cdot 8^2 \cdot 10^2)(6 \cdot 4^8)_2$ topology, but **2** exhibits a 3D open network with the $(4^2 \cdot 5)_2(4 \cdot 4^5 \cdot 10^6 \cdot 8^7 \cdot 4^8)_2$ topology. The solid-state excitation–emission spectra show that the strongest excitation peaks for **1** and **2** are at 341 and 319 nm, and their emission spectra mainly show strong peaks at 410 and 405 nm, respectively. The amounts adsorbed of **1** (**2**) are 169 mg/g (126 mg/g) for H_2O , 137 mg/g (102 mg/g) for C_2H_5OH , and 133 mg/g (99 mg/g) for CH_3OH , which are equivalent to the adsorption of about 62 (34) H_2O , 20 (11) C_2H_5OH , and 28 (16) CH_3OH per unit cell, respectively.

Introduction

The synthesis and characterization of metal–organic frameworks (MOFs) have attracted much attention for their enormous variety of interesting structural topologies and wide potential applications as functional materials, such as porosity, chirality, catalysis, luminescence, magnetism, conductivity, spin-transition (spin-crossover), and nonlinear optics (NLO).^{1–12} Recently, Férey et al. examined the magnetic and sorption properties of a large-pore, flexible, open framework,

$V^{III}(OH)\{O_2C-C_6H_4-CO_2\} \cdot \chi(HO_2C-C_6H_4-CO_2H) \cdot (\chi \sim 0.75)$ (MIL-47).¹³ Li et al. synthesized a thermally stable, nanoporous, organometallic structure, $[Co_3(bpdc)_3(bpy) \cdot 4(DMF) \cdot (H_2O)]$ (IRPM-1), that exhibits a high sorption capacity for large hydrocarbons over a wide temperature range and superior size/shape selectivity for the in situ photolysis of *o*-MeDBK.¹⁴ However, MOFs with multifunctionality are still very rare.

Over the past decade, chiral metal–organic frameworks (MOFs) formed through self-organization using organic solvent under mild conditions have been of intense interest in the coordination chemistry and materials chemistry fields.^{15–23} Several approaches have been previously reported

* To whom correspondence should be addressed. E-mail: sqiu@mail.jlu.edu.cn (S.Q.); zhugs@mail.jlu.edu.cn (G.Z.).

- (1) Batten, S. R.; Robson, R. *Angew. Chem., Int. Ed.* **1998**, *37*, 1460.
- (2) Eddaoudi, M.; Moler, D. B.; Li, H.; Chen, B.; Reineke, T. M.; O'Keeffe, M.; Yaghi, O. M. *Acc. Chem. Res.* **2001**, *34*, 319.
- (3) Janiak, C. *Dalton Trans.* **2003**, 2781.
- (4) Férey, G.; Mellot-Draznieks, C.; Serre, C.; Millange, F.; Dutour, J.; Surlblé, S.; Margiolaki, I. *Science* **2005**, *309*, 2040.
- (5) Zhao, X.; Xiao, B.; Fletcher, A. J.; Thomas, K. M.; Bradshaw, D.; Rossinsky, M. J. *Science* **2004**, *306*, 1012.
- (6) Moulton, B.; Zaworotko, M. J. *Chem. Rev.* **2001**, *101*, 1629.
- (7) Kitagawa, S.; Kitaura, R.; Noro, S. *Angew. Chem., Int. Ed.* **2004**, *43*, 2334.
- (8) Hargman, P. J.; Hargman, D.; Zubieta, J. *Angew. Chem., Int. Ed.* **1999**, *38*, 2639.
- (9) Halder, G. J.; Kepert, C. J.; Moubaraki, B.; Murray, K. S.; Cashion, J. D. *Science* **2002**, *298*, 1762.
- (10) Evans, O. R.; Ngo, H. L.; Lin, W. J. *Am. Chem. Soc.* **2001**, *123*, 10395.
- (11) Fang, Q. R.; Zhu, G. S.; Xue, M.; Sun, J. Y.; Tian, G.; Wu, G.; Qiu, S. L. *Dalton Trans.* **2004**, 2202.

- (12) Fang, Q. R.; Zhu, G. S.; Xue, M.; Sun, J. Y.; Wei, Y.; Qiu, S. L.; Xu, R. R. *Angew. Chem., Int. Ed.* **2005**, *44*, 3845.
- (13) Barthelet, K.; Marrot, J.; Riou, D.; Férey, G. *Angew. Chem., Int. Ed.* **2002**, *41*, 281.
- (14) Pan, L.; Liu, H. M.; Lei, X. G.; Huang, X. Y.; Olson, D. H.; Turro, N. J.; Li, J. *Angew. Chem., Int. Ed.* **2003**, *42*, 542.
- (15) Piguet, C.; Bernardinelli, G.; Hopfgartner, G. *Chem. Rev.* **1997**, *97*, 2005.
- (16) Albrecht, M. *Chem. Rev.* **2001**, *101*, 3457.
- (17) Seo, J. S.; Whang, D.; Lee, H.; Jun, S. I.; Oh, J.; Jeon, Y. J.; Kim, K. *Nature* **2000**, *404*, 982.
- (18) Childs, L. J.; Alcock, N. W.; Hannon, M. J. *Angew. Chem., Int. Ed.* **2001**, *40*, 1097.
- (19) Charbonniere, L. J.; Williams, A. F.; Piguet, C.; Bernardinelli, G.; Rivara-Minten, E. *Chem.—Eur. J.* **1998**, *4*, 485.

for creating chiral materials, including the introduction of chiral ligands or chiral templates, the influence of the chiral physical environment, and the spontaneous resolution without any chiral auxiliary.^{24–28} Usually, spontaneous chiral resolution is a peculiar phenomenon and has been found only occasionally in MOFs.^{29,30} Recently, we synthesized an interesting layer chiral MOF, $\text{Co}(\text{PDC})(\text{H}_2\text{O})_2 \cdot (\text{H}_2\text{O})$, with both right-handed and left-handed helical chains by using achiral ligand pyridine-2,5-dicarboxylic acid (H_2PDC).³¹ As a sequel, we present here two novel 3D chiral microporous (pore diameters $\leq 20 \text{ \AA}$)³² MOFs, $\text{Zn}_3(\text{BTC})_2(\text{DMF})_3(\text{H}_2\text{O}) \cdot (\text{DMF})(\text{H}_2\text{O})$ (**1**) and $\text{Cd}_4(\text{BTC})_3(\text{DMF})_2(\text{H}_2\text{O})_2 \cdot 6(\text{H}_2\text{O})$ (**2**) ($\text{H}_3\text{BTC} = 1,3,5\text{-benzenetricarboxylic acid}$ and $\text{DMF} = N,N'$ -dimethylformamide), built from achiral BTC ligands and different metal–carboxylate clusters ($\text{Zn}(\text{II})$ or $\text{Cd}(\text{II})$). Of particular interest is that **1** is a trinodal (3,4)-connected net with two 4-connected nodes (square and tetrahedral SBUs) and one 3-connected (BTC ligand) node, and its Schläfli symbol is $(6^3)_4(6^2 \cdot 8^2 \cdot 10^2)(6^4 \cdot 8^2)_2$; however, **2** could be described as a binodal (3,8)-connected net with 8-connected (tetranuclear SBU of Cd_4) and 3-connected (BTC ligand) nodes, and its Schläfli symbol is $(4^2 \cdot 5)_2(4 \cdot 4^5 \cdot 10^6 \cdot 8^7 \cdot 4^8)_2$. In addition, the fluorescence and adsorption properties for **1** and **2** have also been examined. To the best of our knowledge, multifunctional MOFs with both fluorescence and adsorption properties are very limited.³³

Experimental Section

Materials and Measurements. All reagents and solvents were commercially available and used as received without further purification. A Perkin–Elmer TGA 7 thermogravimetric analyzer was used to obtain thermogravimetric analysis (TGA) curves in air with a heating rate of $5 \text{ }^\circ\text{C min}^{-1}$. Powder X-ray diffraction (XRD) data were collected on a Siemens D5005 diffractometer with $\text{Cu K}\alpha$ radiation ($\lambda = 1.5418 \text{ \AA}$). Analyses for C, H, and N were carried out on a Perkin–Elmer analyzer. Infrared (IR) spectra were recorded ($400\text{--}4000 \text{ cm}^{-1}$ region) on a Nicolet Impact 410 FTIR spectrometer using KBr pellets. Adsorption measurements were conducted on a CAHN 2000 analyzer at room temperature.

Preparation of $\text{Zn}_3(\text{BTC})_2(\text{DMF})_3(\text{H}_2\text{O}) \cdot (\text{DMF})(\text{H}_2\text{O})$ (1**).** $\text{Zn}(\text{NO}_3)_2 \cdot 6\text{H}_2\text{O}$ (0.03 g, 0.1 mmol), 0.10 g (0.5 mmol) of BTC, 8.0 mL of DMF, 1.0 mL of ethanol (EtOH), and 1.0 mL of H_2O were placed in a 25 mL vial to form a solution under stirring. After stirring the solution in air for 1 h, we set the vial in a beaker (100 mL) containing a DMF solution (5 mL) of tributylamine (TBA, 0.3 mL) and then sealed it and left it undisturbed at $60 \text{ }^\circ\text{C}$ for 3 days. The resulting colorless block-shaped single crystals of **1** were collected in 70% yield on the basis of zinc. The complexes were stable in air and insoluble in common organic solvents such as acetone, methanol, ethanol, dichloromethane, acetonitrile, chloroform, DMF, and DMSO. Elemental anal. Found: C, 38.31; H, 4.22; N, 5.89. Calcd: C, 38.38; H, 4.08; N, 5.97. FT-IR (KBr): $\bar{\nu}$ 3448 (m), 2931 (w), 1658 (w), 1628 (s), 1574 (m), 1442 (m), 1373 (s), 1257 (w), 1103 (m), 933 (w), 856 (w), 764 (m), 725 (m), 571 (w), 540 (w) cm^{-1} .

Preparation of $\text{Cd}_4(\text{BTC})_3(\text{DMF})_2(\text{H}_2\text{O})_2 \cdot 6(\text{H}_2\text{O})$ (2**).** 0.24 g (0.8 mmol) of $\text{Cd}(\text{NO}_3)_2 \cdot 4\text{H}_2\text{O}$ (0.24 g, 0.8 mmol), 0.02 g (0.1 mmol) of BTC, 10.0 mL of DMF, 5.0 mL of EtOH, and 2.0 mL of H_2O were placed in a vial (25 mL) and dissolved under stirring. After stirring the solution in air for 1 h, we set the vial in a beaker (100 mL) containing a DMF solution (5 mL) of triethylamine (TEA, 0.1 mL) and then sealed it and left it undisturbed at $60 \text{ }^\circ\text{C}$ for 3 days. The resulting colorless block-shaped single crystals of **2** were collected in 65% yield on the basis of cadmium. The complexes were stable in air and insoluble in common organic solvents such as acetone, methanol, ethanol, dichloromethane, acetonitrile, chloroform, DMF, and DMSO. Elemental anal. Found: C, 29.73; H, 2.04; N, 1.24. Calcd: C, 29.63; H, 1.99; N, 1.15. FT-IR (KBr): $\bar{\nu}$ 3469 (m), 1612 (s), 1562 (s), 1437 (s), 1375 (s), 1107 (m), 935 (w), 773 (m), 725 (m), 594 (w), 523 (m) cm^{-1} .

Crystal Structure Determination. Diffraction intensities for **1** and **2** were collected on a computer-controlled Bruker SMART CCD diffractometer equipped with graphite-monochromated $\text{Mo K}\alpha$ radiation with radiation wavelength of 0.71073 \AA by using the ω -scan technique. The structures were solved by direct methods and refined with the full-matrix least-squares technique using the program SHELXTL.³⁴ Anisotropic thermal parameters were assigned to all non-hydrogen atoms. The hydrogen atoms were set in calculated positions. The crystallographic data, selected bond lengths, and angles for **1** and **2** are listed in Tables 1–3. CCDC-274240 (**1**) and CCDC-253132 (**2**) contain the supplementary crystallographic data for this paper. These data can be obtained free of charge via www.ccdc.cam.ac.uk/contents/retrieving.html (or from the Cambridge Crystallographic Data Centre, 12 Union Road, Cambridge CB21EZ, U.K.; fax: (44) 1223-336-033; e-mail: deposit@ccdc.cam.ac.uk).

Results and Discussion

Synthesis and Crystal Structures. **1** and **2** were synthesized in the presence of organic bases TBA and TEA, respectively. In a typical procedure for synthesizing **1**, a mixture of $\text{Zn}(\text{NO}_3)_2 \cdot 6\text{H}_2\text{O}$ with BTC was prepared with a 1:5 metal-to-ligand ratio in DMF/EtOH/ H_2O , and a DMF solution of TBA was then allowed to diffuse into the above mixture at $60 \text{ }^\circ\text{C}$ to deprotonate the acid and initiate the copolymerization process. After the reaction solution stood for 3 days, colorless block-shaped crystals of **1** were collected in 70% yield on the basis of zinc. The synthesis of **2** was

- (20) Lehn, J. M. *Supramolecular Chemistry*; VCH: Weinheim, Germany, 1995.
- (21) Xiong, R. G.; You, X. Z.; Abrahams, B. F.; Xue, Z.; Che, C. M. *Angew. Chem., Int. Ed.* **2001**, *40*, 4422.
- (22) Sun, J. Y.; Weng, L. H.; Zhou, Y. M.; Chen, J. X.; Chen, Z. X.; Liu, Z. C.; Zhao, D. Y. *Angew. Chem., Int. Ed.* **2002**, *41*, 4471.
- (23) Lin W. B. *J. Solid State Chem.* **2005**, *178*, 2486.
- (24) Shi, X.; Zhu, G. S.; Qiu, S. L.; Huang, K. L.; Yu, J. H.; Xu, R. R. *Angew. Chem., Int. Ed.* **2004**, *43*, 6482.
- (25) Carlucci, L.; Ciani, G.; Proserpio, D. M.; Rizzato, S. *Chem. Commun.* **2000**, 1319.
- (26) Ranford, J. D.; Vittal, J. J.; Wu, D.; Yang, X. *Angew. Chem., Int. Ed.* **1999**, *38*, 3498.
- (27) Ezuhara, T.; Endo, K.; Aoyama, Y. *J. Am. Chem. Soc.* **1999**, *121*, 3279.
- (28) Biradha, K.; Seward, C.; Zaworotko, M. J. *Angew. Chem., Int. Ed.* **1999**, *38*, 492.
- (29) Jacques, J.; Collet, A.; Wilen, S. H. *Enantiomers, Racemates and Resolutions*; Krieger Publishing Company: Malabar, FL, 1994.
- (30) Pérez-García, L.; Amabilino, D. B. *Chem. Soc. Rev.* **2002**, *31*, 342.
- (31) Tian, G.; Zhu, G. S.; Yang, X. Y.; Fang, Q. R.; Xue, M.; Sun, J. Y.; Wei, Yan; Qiu, S. L. *Chem. Commun.* **2005**, 1396.
- (32) *IUPAC Manual of Symbols and Terminology*, Appendix 2, Part I, Colloid and Surface Chemistry; *Pure Appl. Chem.* **1972**, *31*, 578.
- (33) Reineke, T. M.; Eddaoudi, M.; Fehr, M.; Kelley, D.; Yaghi, O. M. *J. Am. Chem. Soc.* **1999**, *121*, 1651.

- (34) Sheldrick, G. M. *SHELXTL Version 5.1 Software Reference Manual*; Bruker AXS, Inc.: Madison, WI, 1997.

Table 1. Data Collection and Processing Parameters for **1** and **2**

	1	2
formula	C ₃₀ H ₃₈ N ₄ O ₁₈ Zn ₃	C ₃₃ H ₃₉ N ₂ O ₂₈ Cd ₄
fw	938.79	1361.31
T (K)	293(2)	293(2)
cryst syst	tetragonal	tetragonal
space group	P4 ₁ 2 ₁ 2	P4 ₃ 22
a (Å)	13.6929(19)	10.3503(4)
c (Å)	50.664(10)	52.557(3)
V (Å ³)	9499(3)	5630.4(4)
Z	8	4
ρ (g/cm ³)	1.307	1.483
μ (mm ⁻¹)	1.567	1.555
F(000)	3808	2428
Flack param	0.38(2)	-0.02(5)
θ (deg)	1.21–28.22	1.97–28.14
index ranges	-13 ≤ h ≤ 17, -18 ≤ k ≤ 18, -64 ≤ l ≤ 56	-12 ≤ h ≤ 13, -13 ≤ k ≤ 13, -54 ≤ l ≤ 69
no. of reflns. collected	58564	34228
no. of ind. reflns.	11110	6540
data/restraints/params	11110/52/496	6540/41/282
GOF on F ²	1.079	1.015
R ₁ , ^a wR ₂ ^b [I > 2σ(I)]	0.0761, 0.2000	0.0417, 0.1234
R ₁ , wR ₂ (all data)	0.1081, 0.2191	0.0460, 0.1256
largest diff. peak and hole (e Å ⁻³)	1.611 and -0.520	1.698 and -0.600

$${}^a R_1 = \sum ||F_o| - |F_c||/|F_o|, {}^b wR_2 = [\sum w(F_o^2 - F_c^2)^2 / \sum w(F_o^2)^2]^{1/2}.$$

Table 2. Selected Bond Lengths (Å) and Angles (deg) for **1**^a

Zn(1)–O(11A)	1.988(3)	Zn(2)–O(9D)	2.067(3)
Zn(1)–O(7)	2.003(3)	Zn(2)–Zn(2C)	2.9550(10)
Zn(1)–O(1)	2.036(3)	Zn(3)–O(12A)	2.048(3)
Zn(1)–O(6B)	2.041(3)	Zn(3)–O(14)	2.046(4)
Zn(1)–O(5B)	2.405(4)	Zn(3)–O(17)	2.067(4)
Zn(2)–O(15)	1.976(3)	Zn(3)–O(8)	2.130(3)
Zn(2)–O(10B)	1.987(4)	Zn(3)–O(1)	2.135(3)
Zn(2)–O(3C)	2.049(4)	Zn(3)–O(13)	2.167(4)
Zn(2)–O(4)	2.065(3)		
O(7)–Zn(1)–O(1)	103.84(13)	O(17)–Zn(3)–O(1)	92.00(16)
O(15)–Zn(2)–O(4)	102.61(14)	O(8)–Zn(3)–O(1)	92.31(13)
O(14)–Zn(3)–O(17)	88.48(18)	O(14)–Zn(3)–O(13)	91.14(16)
O(14)–Zn(3)–O(8)	87.34(15)	O(17)–Zn(3)–O(13)	86.48(19)
O(17)–Zn(3)–O(8)	172.66(17)	O(8)–Zn(3)–O(13)	87.57(16)
O(14)–Zn(3)–O(1)	178.66(14)	O(1)–Zn(3)–O(13)	90.14(14)

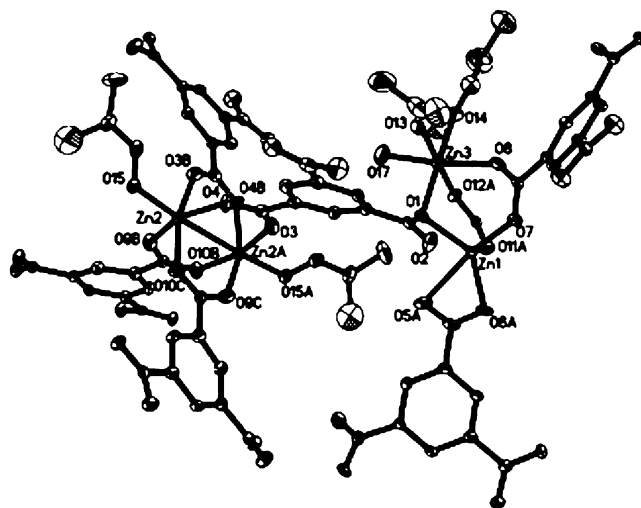
^a Transformations were as follows: A = -x + 5/2, y + 1/2, -z + 1/4; B = x + 3/2, y + 1/2, -z + 1/4; C = -y + 1, -x + 1, -z + 1/2; D = -y + 1/2, x - 1/2, z + 1/4.

Table 3. Selected Bond Lengths (Å) and Angles (deg) for **2**^a

Cd(1)–O(9A)	2.217(5)	Cd(2)–O(10)	2.318(7)
Cd(1)–O(1)	2.245(4)	Cd(2)–O(11)	2.300(6)
Cd(1)–O(2B)	2.255(4)	Cd(2)–O(8)	2.350(4)
Cd(1)–O(7)	2.309(4)	Cd(2)–O(6C)	2.405(4)
Cd(1)–O(5C)	2.363(4)	Cd(2)–O(7)	2.427(4)
Cd(1)–O(6C)	2.415(4)	Cd(2)–O(3D)	2.449(5)
Cd(2)–O(4D)	2.273(4)		
O(1)–Cd(1)–O(7)	92.68(15)	O(10)–Cd(2)–O(7)	87.8(2)
O(10)–Cd(2)–O(11)	170.2(3)	O(11)–Cd(2)–O(7)	81.6(2)
O(10)–Cd(2)–O(8)	85.2(3)	O(8)–Cd(2)–O(7)	54.28(14)
O(11)–Cd(2)–O(8)	88.2(3)		

^a Transformations were as follows: A = x, y + 1, z; B = -x + 1, y, -z + 2; C = -x, y, -z + 2; D = y - 1, -x + 1, z + 1/4.

the same as that for **1** but substituting Cd(NO₃)₂·4H₂O for Zn(NO₃)₂·6H₂O and TEA for TBA, respectively; the yield was 65% on the basis of cadmium. Though not observed in the crystalline structure, TBA and TEA can play deprotonating reagents and some structure-directing role.³⁵ The control reaction without using TBA for **1** but using another base (such as TEA) instead will result in another 3D

**Figure 1.** ORTEP drawing (at a 50% probability level) of the coordination environment of zinc ions in **1**. (For clarity, the H atoms and one BTC molecule, except for a carboxylate group, are not shown.)

compound³⁶ under the same conditions. Similarly, the synthesis without using TEA for **2** but using another base (such as TBA) will result in a new 1D compound.³⁷ The complexes of **1** and **2** were stable in air and insoluble in common organic solvents such as acetone, methanol, ethanol, dichloromethane, acetonitrile, chloroform, DMF, and DMSO.

X-ray crystallography reveals that **1** crystallizes in a chiral space group P4₁2₁2 (No. 92) and consists of a 3D open framework with the (6³)₄(6²·8²·10²)(6⁴8²)₂ topology.³⁸ The fundamental building unit of **1** contains four zinc ions, seven crystallographically equivalent BTC ligands, four DMF, and one H₂O (Figure 1). The Zn1 center is coordinated by five oxygen atoms (O1, O5A, O6A, O7, and O11A) from four different BTC ligands. The Zn3 center adopts distorted octahedral coordination geometries with six oxygen atoms from three different BTC ligands (O1, O8, and O12A), two DMF (O13 and O14), and one H₂O (O17). The Zn1 and Zn3 centers are bridged through three carboxylate groups to construct tetrahedral secondary building units (SBUs). Different from Zn1 and Zn3 centers, Zn2 and Zn2A centers are linked by four carboxylate groups (O3, O3A, O4, O4A, O9B, O9C, O10B, and O10C) from four distinct BTC ligands into the paddle-wheel cluster motif, and each of them completes its octahedral coordination geometries with an axial DMF (O15 or O15A) opposite to the Zn–Zn vector. Clearly, Zn2 and Zn2A centers coordinated to four carboxylate groups can act as square SBUs. In addition, the dihedral angles of

(35) Tian, Y. Q.; Cai, C. X.; Ji, Y.; You, X. Z.; Peng, S. M.; Lee, G. H. *Angew. Chem., Int. Ed.* **2002**, *41*, 1384.

(36) Crystal data for Zn₃O(BTC)₂(DMF): C₂₁H₁₃Zn₃NO₁₄, Mr = 699.47, space group *I4* cm, tetragonal, a = 20.4518(13) Å, c = 17.813(2) Å, V = 7451.0(12) Å³, Z = 8, D_c = 1.276 g cm⁻³, μ(Mo–Kα) = 1.969 mm⁻¹, F(000) = 2848, the final R (wR₂) = 0.0509 (0.1450) for 3608 reflections with I ≥ 2σ(I).

(37) Crystal data for Cd₂(BTC)₄(H₂O)₄·23(H₂O): C₃₆H₆₆Cd₂O₅₁, Mr = 1539.71, space group *P1*, triclinic, a = 9.6670 Å, b = 10.0954 Å, c = 16.3370 Å, α = 81.249°, β = 77.640°, γ = 69.635°, V = 1454.81(15) Å³, Z = 1, D_c = 1.695 g cm⁻³, μ(Mo–Kα) = 0.855 mm⁻¹, F(000) = 732, the final R (wR₂) = 0.048 (0.1315) for 5845 reflections with I ≥ 2σ(I).

(38) Although we did not find its enantiomer, the bulk of **1** should be racemic and may contain both P4₁2₁2 and P4₃2₁2 crystals.

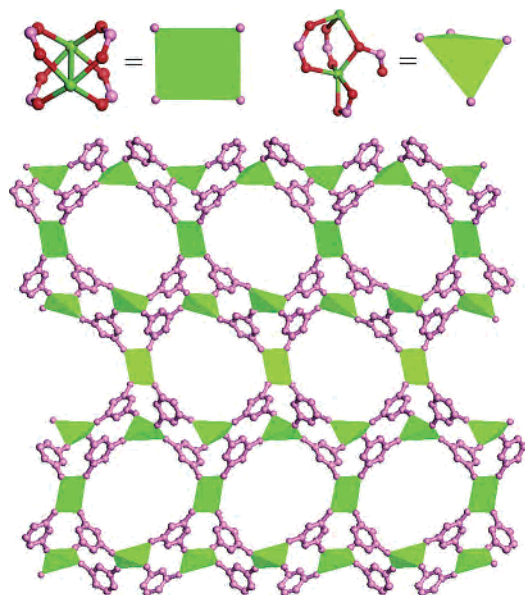


Figure 2. View along the [100] direction showing elliptical channels with about $9.6 \times 11.9 \text{ \AA}^2$ of **1**. The square and tetrahedral SBUs built from two zinc centers and four carboxylate groups of BTC ligands are shown at the top left and right corners, respectively. The color code: Zn, green; O, red; C, pink.

BTC ligands between benzene rings and their carboxylate groups are between 9.4 and 39.2° in **1**, which is apparently induced by their coordinated forms. The tetrahedral and square SBUs are interconnected by distorted BTC ligands, thereby generating a 3D chiral extended network with elliptical channel dimensions of ca. $9.6 \times 11.9 \text{ \AA}^2$ (measured between opposite atoms) viewed along the [100] or [010] directions (Figure 2); the void space is filled with three coordinated DMF, one coordinated H_2O , one guest DMF, and one guest H_2O , as established by elemental analysis and thermogravimetric analysis (TGA).³⁹ The effective free volume of **1** is calculated by PLATON analysis⁴⁰ as being 22.5% (0.17 mL/g) of the crystal volume (2137 \AA^3 out of the 9499 \AA^3 unit cell volume). When removing DMF and H_2O molecules, we computed its effective free volume as being 24% (0.18 mL/g) by PLATON analysis of the crystal volume (2278 \AA^3 out of the 9499 \AA^3 unit cell volume).

A better insight into the nature of the involuted framework can be achieved by the application of a topological approach, i.e., reducing multidimensional structures to simple node-and-connection nets. As discussed above, square SBUs (Zn2 and Zn2A centers) and tetrahedral SBUs (Zn1 and Zn3 centers) are defined as 4-connected nodes. Likewise, BTC ligands ligating with three SBUs (square or tetrahedral) can act as 3-connected nodes. On the basis of the simplification principle, the resulting structure of compound **1** is a trinodal (3,4)-connected net with two 4-connected nodes (square and

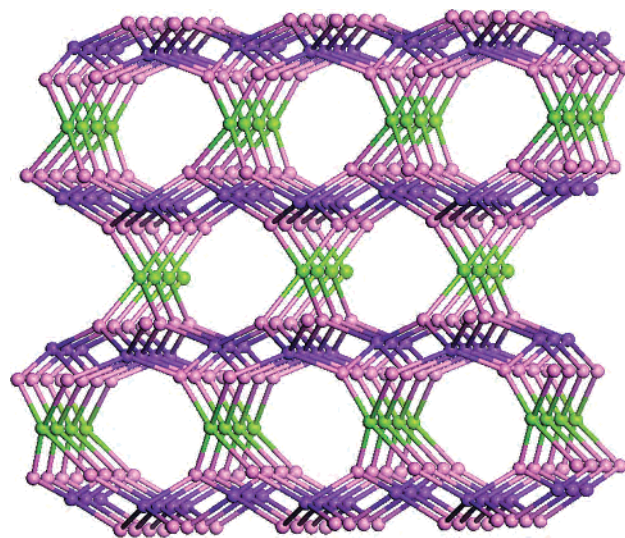


Figure 3. Schematic illustration of the $(6^3)_4(6^2 \cdot 8^2 \cdot 10^2)(6 \cdot 48^2)_2$ topology of the 3D network of **1**. Color code: green balls, square SBUs; purple balls, tetrahedral SBUs; pink balls, 3-connected BTC ligands.

tetrahedral SBUs) and one 3-connected (BTC ligand) node, and its Schläfli symbol is $(6^3)_4(6^2 \cdot 8^2 \cdot 10^2)(6 \cdot 48^2)_2$ (the first symbol represents the BTC ligand, the second the square SBU, and the third the tetrahedral SBU; Figure 3).^{41–44}

The structure determination of **2** shows that it is not enantiopure but a case of twinning by inversion with Flack 0.38 (space group $P4_322$, No. 95) and exhibits a 3D open network with the $(4^2 \cdot 5)_2(4 \cdot 4^5 \cdot 10 \cdot 6 \cdot 8^7 \cdot 4^8^2)$ topology.⁴⁵ The fundamental building unit of **2** contains two cadmium ions, six crystallographically equivalent BTC ligands, one DMF, and one H_2O (Figure 4). The Cd1 center adopts a distorted octahedral coordination geometry with six oxygen atoms (O1, O2A, O5B, O6B, O7, and O9A) from five distinct BTC ligands occupying each coordination site. The Cd2 center is coordinated by seven oxygen atoms: five (O3C, O4C, O6B, O7, and O8) from three different BTC ligands, one (O10) from DMF, and one (O11) from H_2O . In this structure, the dihedral angles of BTC ligands are between 4.3 and 23.0° . Interestingly, two types of pores with diameters of about 4.1 and 7.2 \AA around the cadmium atoms are formed on those 4_3 screw axes at the origin and face center of each unit cell, respectively, and the middle sections of those pores are filled with BTC ligands (Figure 5) viewed along the [001] direction. In addition, those distorted BTC ligands coordinated to cadmium ions build up the 3D open framework of **2** with elliptical channels of ca. $6.4 \times 11.3 \text{ \AA}^2$ (measured between opposite atoms) viewed along the [100] or [010] directions (Figure 6), and the vacancies are filled with two coordinated DMF, two coordinated H_2O , and six guest

(39) The TGA curve for **1** shows that the weight loss of 9.63% during the first step between 80 and $130 \text{ }^\circ\text{C}$ corresponds to the loss of a guest H_2O and a guest DMF (calculated 9.71%), and the weight loss of 25.26% during the second step between 150 and $315 \text{ }^\circ\text{C}$ corresponds to the loss of one coordinated H_2O and three coordinated DMF (calculated 25.28%). Decomposition of **1** began above $400 \text{ }^\circ\text{C}$. The residue was ZnO (experimental = 26.02% and calculated = 26.00%).
 (40) van der Sluis, P.; Spek, A. L. *Acta Crystallogr., Sect. A* **1990**, *46*, 194.

(41) Wells, A. F. *Further Studies of Three-Dimensional Nets*; American Crystallographic Association (distributed by Polycrystal Book Service): New York (Pittsburgh, PA), 1979.
 (42) Wells, A. F. *Three-Dimensional Nets and Polyhedra*; Wiley: New York, 1977.
 (43) Blake, A. J.; Champness, N. R.; Hubberstey, P.; Li, W. S.; Withersby, M. A.; Schröder, M. *Coord. Chem. Rev.* **1999**, *183*, 117.
 (44) Delgado-Friedrichs, O.; O'Keefe, M.; Yaghi, O. M. *Acta Crystallogr., Sect. A* **2003**, *59*, 22.
 (45) Although we did not find its enantiomer, the bulk of **2** should also be racemic and may contain both $P4_322$ and $P4_222$ crystals.

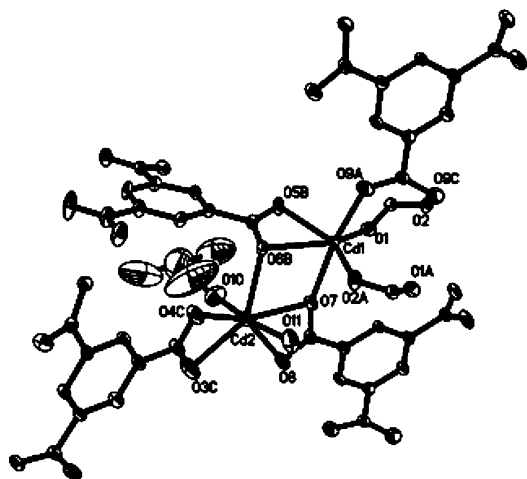


Figure 4. ORTEP drawing (at a 50% probability level) of the coordination environment of cadmium ions in **2**. (For clarity, the H atoms and two BTC molecules, except for two carboxylate groups, are not shown.)

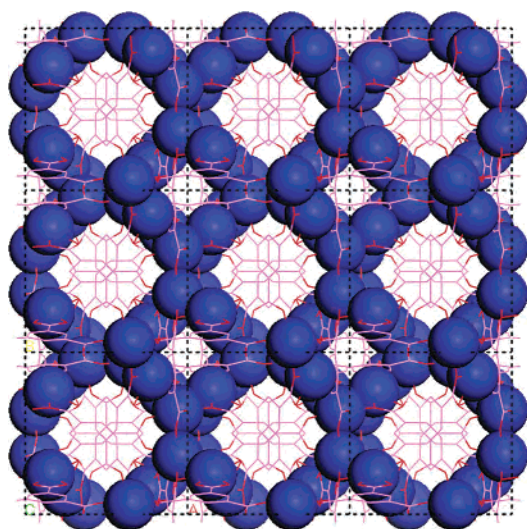


Figure 5. Packing diagram of **2** viewed along the [001] direction. Color code: Cd, blue (ball); O, red; C, pink.

H₂O, as established by elemental analysis and TGA.⁴⁶ By PLATON analysis, we calculated the effective free volume of **2** as being 36.6% (0.25 mL/g) of the crystal volume (2063 Å³ out of the 5630 Å³ unit cell volume), and the effective free volume reaches 41.8% (0.28 mL/g) of the crystal volume (2356 Å³ out of the 5630 Å³ unit cell volume) without DMF and H₂O molecules.

As shown in Figures 6 and 7, one tetranuclear SBU (Cd₂.Cd₁.Cd₁.Cd₂) is surrounded by 12 molecules, i.e., 8 BTC, 2 DMF, and 2 water ligands. As they are end-capping units, 2 DMF and 2 water ligands are disregarded from a topological perspective; this, therefore, defines the tetranuclear SBU as an 8-connected node. In addition, two of eight BTC ligands bridge two tetranuclear SBUs, and other BTC ligands serve as 3-connected nodes. In this structure, the ratio of 3-connected BTC and tetranuclear SBU is 2:1. So the resulting structure of compound **2** is a binodal (3,8)-connected net with the Schläfli symbol (4²·5)₂(4⁴·5¹⁰·6⁸·7⁴·8²) (the first symbol is for 3-connected BTC and the second for tetranuclear SBU).

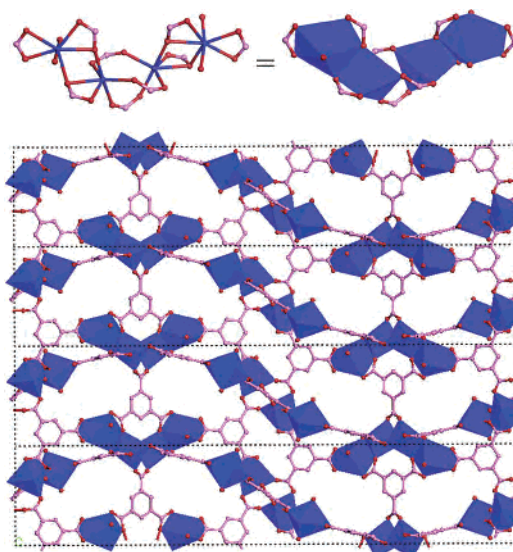


Figure 6. Infinite three-dimensional coordination framework of **2** with elliptical channels of about 6.4 × 11.3 Å² viewed along the [100] direction. The tetranuclear SBUs built from four cadmium centers, eight BTC ligands (exhibiting only their coordinated carboxylate groups), two DMF (exhibiting only their oxygen atoms), and two H₂O are shown at the top. Color code: Cd, blue; O, red; C, pink.

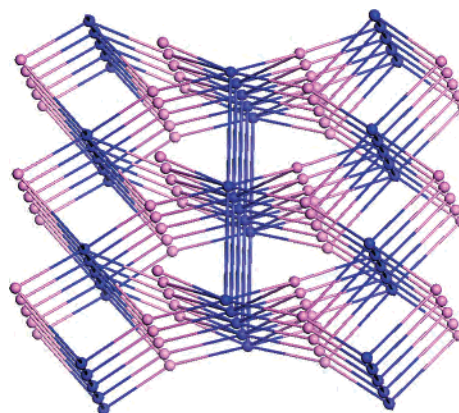


Figure 7. Schematic illustration of the (4²·5)₂(4⁴·5¹⁰·6⁸·7⁴·8²) topology of the 3D network of **2**. Color code: blue balls, 8-connected SBUs; blue lines, bridging BTC ligands; pink balls, 3-connected BTC ligands.

Fluorescence Properties. The solid-state excitation–emission spectra of **1** and **2** have been studied at room temperature (Figure 8). The strongest emission peak for the free BTC is at 370 nm with the excitation peak at 334 nm. It is attributed to the π* → n transitions.⁴⁷ Compared with the free BTC, the strongest excitation peaks for **1** and **2** are at 341 and 319 nm, and their emission spectra mainly show strong peaks at 410 and 405 nm, respectively. The emissions of **1** and **2** are very similar to the free ligand transitions and may be chiefly ligand-centered electronic transitions perturbed by the coordination to metal ions rather than to protons. The difference in their emissions is probably due to the differences in metal ions and coordination environment

(46) The TGA curve of **2** shows that the weight loss of 21.35% from 30 to 260 °C is attributed to the loss of six guest H₂O, two coordinated H₂O, and two coordinated DMF (calculated 21.33%). Decomposition of **2** began at about 330 °C. The residue was CdO (experimental = 37.65% and calculated = 37.73%).

(47) Chen, W.; Wang, J. Y.; Chen, C.; Yue, Q.; Yuan, H. M.; Chen, J. S.; Wang, S. N. *Inorg. Chem.* **2003**, *42*, 944.

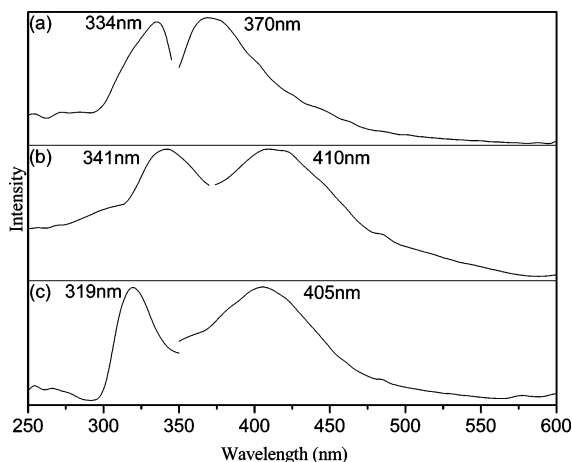


Figure 8. Solid-state excitation–emission spectra of (a) the free BTC, (b) **1**, and (c) **2** at room temperature.

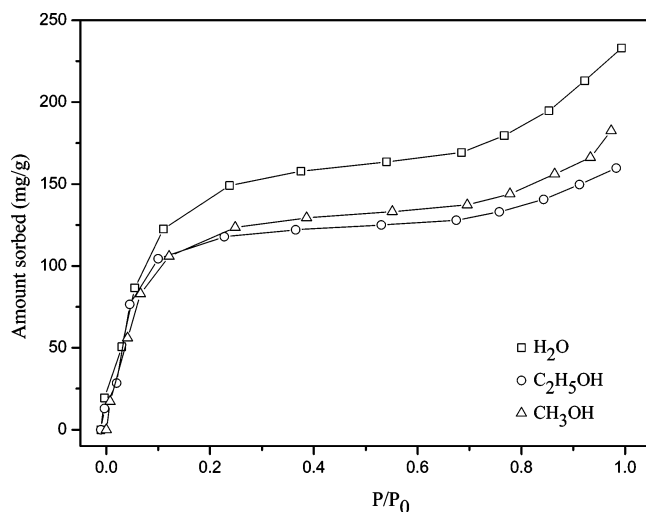


Figure 9. Adsorption isotherms for **1** at room temperature.

around them, because the photoluminescence behavior is closely associated with the metal ions and the ligands coordinated around them.^{48,49} These observations suggest that polymers **1** and **2** will be candidates for potential photoactive material.^{50,51}

Adsorption Properties. The adsorption isotherms for **1** and **2** were also measured at room temperature. Before the measurement, the samples of **1** and **2** were soaked in CH_2Cl_2 for 48 h and then heated at 80 °C for 6 h to remove the included solvent molecules. The powder X-ray diffraction patterns of exchanged products for **1** and **2** were identical to those of their as-synthesized polymers, only with weakened intensities. As shown in Figures 9 and 10, type I behaviors in the range $P/P_0 = 0\text{--}0.6$ are observed for the adsorption isotherms of **1** and **2**, which clearly indicate that incoming guests can move freely into the channels and that the frameworks maintain their rigidity and porosity throughout

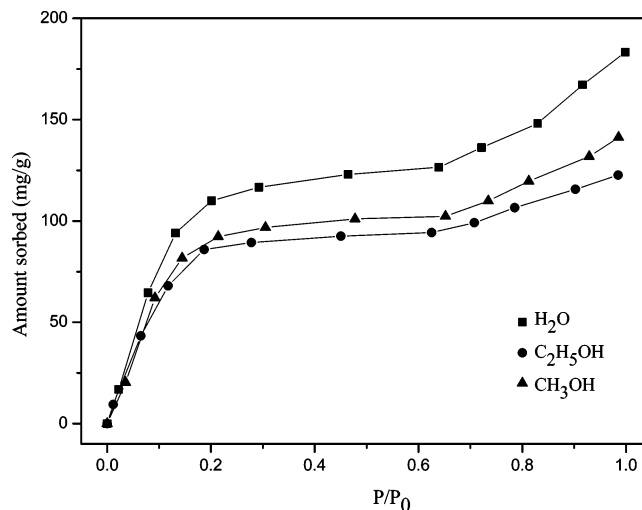


Figure 10. Adsorption isotherms for **2** at room temperature.

the process. The second augments of the amounts adsorbed for **1** and **2** in the range $P/P_0 > 0.6$ can be attributed to adsorption on the external crystallite surface.⁵² At the first saturation, the amounts of **1** adsorbed are 169 mg/g for H_2O , 137 mg/g for $\text{C}_2\text{H}_5\text{OH}$, and 133 mg/g for CH_3OH , which are equivalent to the adsorption of about 62 H_2O , 20 $\text{C}_2\text{H}_5\text{OH}$, and 28 CH_3OH per unit cell, and the amounts sorbed of **2** are 126 mg/g for H_2O , 102 mg/g for $\text{C}_2\text{H}_5\text{OH}$, and 99 mg/g for CH_3OH , which are equivalent to the adsorption of about 34 H_2O , 11 $\text{C}_2\text{H}_5\text{OH}$, and 16 CH_3OH per unit cell. It is worth noting that each of the solvents examined occupies the approximate crystal free volume (0.17 mL/g for **1** and 0.13 mL/g for **2**) as measured at the plateau region. Compared with their calculated free volumes by PLATON program, the free volume of **1** is similar to its calculated value (0.18 mL/g) but the free volume of **2** is less than its calculated value (0.28 mL/g), because **2** has collapsed partially after being heated at 80 °C for 6 h to remove the included solvent molecules.

In conclusion, we have successfully synthesized two new 3D chiral microporous MOFs, $\text{Zn}_3(\text{BTC})_2(\text{DMF})_3(\text{H}_2\text{O}) \cdot (\text{DMF})(\text{H}_2\text{O})$ (**1**) with $(6^3)_4(6^2 \cdot 8^2 \cdot 10^2)(6 \cdot 4^8)_2$ topology and $\text{Cd}_4(\text{BTC})_3(\text{DMF})_2(\text{H}_2\text{O})_2 \cdot 6(\text{H}_2\text{O})$ (**2**) with $(4^2 \cdot 5)_2 \cdot (4 \cdot 4^5 \cdot 10^6 \cdot 8^7 \cdot 4^8)_2$ topology, constructed from achiral BTC ligands coordinated to zinc or cadmium ions in the presence of organic bases TBA and TEA, respectively. In addition, these two MOFs exhibit both fluorescence properties and substantial adsorption behaviors.

Acknowledgment. This research was supported by grants from the State Basic Research Project (G2000077507) and the National Natural Science Foundation of China (Grants 29873017, 20273026, and 20101004).

Supporting Information Available: Crystallographic data in CIF format, IR spectra, powder X-ray patterns, TGA for **1** and **2**. This material is available free of charge via the Internet at <http://pubs.acs.org>.

IC051810K

(48) Zhang, L. Y.; Liu, G. F.; Zheng, S. L.; Ye, B. H.; Zhang, X. M.; Chen, X. M. *Eur. J. Inorg. Chem.* **2003**, 2965.
 (49) Dai, J. C.; Wu, X. T.; Fu, Z. Y.; Cui, C. P.; Wu, S. M.; Du, W. X.; Wu, L. M.; Zhang, H. H.; Sun, Q. *Inorg. Chem.* **2002**, *41*, 1391.
 (50) Wang, X. L.; Qin, C.; Li, Y. G.; Hao, N.; Hu, C. W.; Xu, L. *Inorg. Chem.* **2004**, *43*, 1850.
 (51) Fang, Q. R.; Zhu, G. S.; Shi, X.; Wu, G.; Tian, G.; Wang, R. W.; Qiu, S. L. *J. Solid State Chem.* **2004**, *177*, 1060.

(52) Eddaoudi, M.; Li, H. L.; Yaghi, O. M. *J. Am. Chem. Soc.* **2000**, *122*, 1391.